

# Highly Ordered Honeycomb Film Formation of Linear Polymers by the Breath Figure Technique

Paul A. Gurr,<sup>A,C</sup> Zhou Zhang,<sup>A,B,C</sup> Xiaojuan Hao,<sup>B</sup>  
Timothy C. Hughes,<sup>B,D</sup> and Greg G. Qiao<sup>A,D</sup>

<sup>A</sup>Polymer Science Group (PSG), Department of Chemical and Biomolecular Engineering, The University of Melbourne, Parkville, Vic. 3010, Australia.

<sup>B</sup>Manufacturing, Commonwealth Scientific and Industrial Research Organisation (CSIRO), Clayton, Vic. 3168, Australia.

<sup>C</sup>P.A. Gurr and Z. Zhang are equally first authors.

<sup>D</sup>Corresponding authors. Email: [gregghq@unimelb.edu.au](mailto:gregghq@unimelb.edu.au); [Tim.Hughes@csiro.au](mailto:Tim.Hughes@csiro.au)

Highly ordered, porous honeycomb (HC) films were prepared by the breath figure technique from linear polymers poly (methyl methacrylate) (PMMA) and polystyrene (PS). Typically HC films are difficult to form from such simple linear polymers. The addition of a novel fluorinated polymer (FP) additive with as little as 1 wt-% to PMMA or 5 wt-% to PS was required to obtain regular porous HC films. Through investigation of the influence of the additive on the polymer properties, three parameters based on interfacial tension, polymer solution viscosity, and polymer solidification rate were identified as key factors affecting the ability of polymer systems to form regular porous HC films. A new hypothesis was subsequently developed based on the relationships of these parameters to explain the unusual behaviour associated with HC film formation from linear PMMA and PS with addition of FP additive. This work will provide a new tool to guide the formation of HC films and will greatly broaden the range of polymers used to form HC films in the future.

Manuscript received: 26 February 2016.

Manuscript accepted: 25 March 2016.

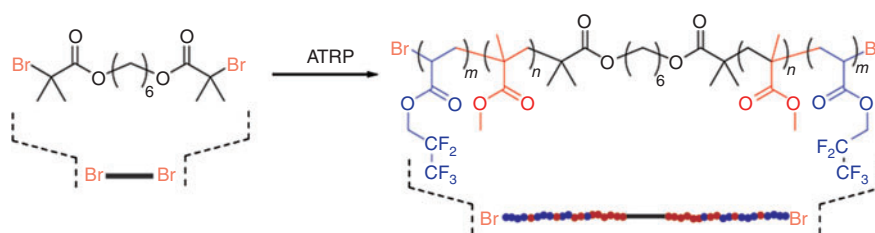
Published online: 20 May 2016.

## Introduction

A wide range of polymer architectures have been used with the breath figure technique to achieve ordered macroporous and microporous structures, such as rod-coil block copolymers,<sup>[1–3]</sup> photo-responsive block-copolymers,<sup>[4]</sup> conjugated polymers,<sup>[5]</sup> amphiphiles,<sup>[6–8]</sup> dendronized polymers,<sup>[9]</sup> supramolecular structures,<sup>[10]</sup> star polymers,<sup>[11–13]</sup> core cross-linked star polymers,<sup>[14–18]</sup> polyoxometalates,<sup>[19]</sup> small molecules,<sup>[20]</sup> or linear polymers, which were added to water surfaces pre-treated with surfactants.<sup>[21–23]</sup> Despite extensive studies, which include a recent review on the application of ordered honeycomb (HC) films,<sup>[24]</sup> there are currently no theories that can aid with the design of polymers capable of forming ordered HC films.<sup>[25]</sup> In general, only branched polymers or polymers with a high degree of interaction between the chains, such as amphiphilic block copolymers, are capable of forming HC films. Thus, the pool of available polymers capable of forming HC films is relatively small. It is generally believed that the formation of HC films from linear homopolymers is difficult.<sup>[26]</sup> Many commercially available and commonly used linear polymers, such as poly (methyl methacrylate) (PMMA) and polystyrene (PS), which have many industrial applications, are not suitable for forming HC structures outside the narrow molecular weight ranges. Zhu et al.<sup>[7,27]</sup> reported that the use of PS with hydrophobic end groups enabled the formation of HC films; however, the incorporation of commercial non-functionalized PS was not reported. Peng et al.<sup>[28,29]</sup> reported that usage of non-functionalized linear

PMMA ( $M_w = 102.6$  kDa) and PS ( $M_w = 223.2$  kDa) of a particular molecular weight range enabled the formation of HC patterns under humid conditions. However, the molecular weight ( $M_w$ ) of PS was limited to a narrow range between 100 and 400 kDa, whereas that of PMMA was limited between 100 and 2000 kDa. Similarly, Wan et al.<sup>[30]</sup> reported HC formation from commercial PS (235 kDa) with reference to the membrane-forming window being very narrow. It was not clear as to why linear polymers outside of these ranges were unsuitable for forming HC films. This leads to two fundamental questions. What are the driving forces for controlling the formation of HC films? Why are linear polymers, in general, not suited for forming HC films? It remains a great challenge to find a system whereby common polymers can be manipulated to allow for facile HC film formation.

With these challenges in mind, several researchers have investigated the effect of various additives on the polymer solutions ability to form HC films via the breath figure method. HC films of PS were reported to be improved with the addition of poly(styrene)-*co*-poly(glycan),<sup>[31]</sup> amphiphilic block copolymer of PS,<sup>[32]</sup> commercial surfactants,<sup>[33]</sup> and hydrophilic additives including poly(*N,N*-dimethylaminoethyl methacrylate), poly (ethylene glycol) (PEG), and poly(*N*-vinyl pyrrolidone).<sup>[34]</sup> The regularity of the pores in HC films of poly(lactic-*co*-glycolic acid) was significantly improved upon the addition of 10 wt-% PEG<sup>[35]</sup> and phospholipid dioleoylphosphatidylethanolamine.<sup>[36]</sup> In some cases, the additive is present in sufficient quantities to



**Scheme 1.** Synthesis of fluorinated polymer **FP**.

effectively act as a template for a non-HC film-forming polymer.<sup>[37,38]</sup> However, as observed in all previous reports, a significant amount of the additive (typically greater than 20 wt-%) is required to enable successful HC film formation, thereby significantly altering the inherent properties of the polymer.

In this study, we report a unique and effective additive that is capable of facilitating the formation of highly regular HC films at very low incorporation ratios from polymers that would ordinarily be unable to form HC films. A simple fluorinated additive, **FP**, was synthesized and found to facilitate the formation of HC films from common linear polymers such as PMMA and PS. We discovered that 1–5 wt-% of the additive was needed to enable PMMA or PS to form regular HC films. Through an extensive study of the additive system, we have identified three physical material properties, which are changed with the addition of **FP**, and their relationships to one another, which are the likely driving forces for HC film formation. Based on our study, we propose a new insight into how changes in physical material properties can influence the fabrication of a regular HC film. Our experimental discovery can potentially be used to guide the formation of HC structures from a wider range of polymers, which cannot form HC films using existing methods.

## Results and Discussion

### Synthesis of Fluorinated Polymeric Additive

Our previous study on non-cracking HC film suggests that increasing the fluorine content in a polymer could lead to the formation of non-planar HC patterned films with no surface cracking.<sup>[39]</sup> Therefore, an extension of that study was to use a fluorinated polymer **FP** as an additive, which was added to linear PMMA and PS, and to investigate its influence on HC film formation on planar surfaces. Indeed, Pilati<sup>[40]</sup> and de León<sup>[41]</sup> demonstrated that fluorinated block copolymers were able to aid the formation of ordered HC films of poly(ethylene terephthalate) and PS, respectively. Herein, a linear **FP** was synthesized as shown in **Scheme 1**. A difunctional initiator was employed to initiate the copolymerization of 2,2,3,3,3-pentafluoropropylacrylate (PFPA) and MMA via atom transfer radical polymerization (ATRP),<sup>[42]</sup> thus forming a linear gradient **FP**, as a result of differences in the monomer reactivity ratios. **FP** with a fluorine content ( $F$ ) of 80 mol-% was characterized by <sup>1</sup>H NMR and gel permeation chromatography multi-angle-laser-light scattering (GPC-MALLS) (**Table 1**). Linear PMMA was synthesized through free radical polymerization, whereas a commercial linear PS was obtained from Aldrich; their characterization is detailed in **Table 1**.

### Breath Figure Films from Linear PMMA, PS, and Linear Gradient Fluorinated Polymer (FP) as Additive

Initially, we investigated the HC formation behaviour of homopolymers PMMA and PS. HC film formation from linear

**Table 1.** Characterization of fluorinated polymer **FP**, homopolymers PMMA and PS, and polymer sample **B1<sub>1</sub>** (PMMA + 1 wt-% **FP**)

Polymer	$M_w^A$ [kDa]	PDI <sup>A</sup>	PFPA <sup>B</sup> Content [mol-%]	$T_g^C$ [°C]	$E^D$ [GPa]
<b>FP</b>	18.5	1.34	80	–	–
PMMA	8.4	1.45	–	122.3	6.95
PS	30	1.01	–	95.0	5.96
<b>B1<sub>1</sub></b>	–	–	<1	99.8	4.76

<sup>A</sup>Weight-average molecular weight and polydispersity (PDI) of polymers determined by GPC-MALLS and based upon the assumption of 100% mass recovery.

<sup>B</sup>PFPA content determined via <sup>1</sup>H NMR spectroscopic analysis.

<sup>C</sup>Glass transition temperatures determined by DSC at a heating rate of 10°C min<sup>-1</sup>, with values taken from the second heating cycle.

<sup>D</sup>Elastic modulus ( $E$ ) determined by AFM in force mode using the Hertzian contact mechanics model.

PMMA and PS solely has typically been problematic according to previous studies<sup>[28,29]</sup> and is very much dependent on the molecular weights of PMMA and PS. Polymers with molecular weights of less than 100 kDa could not generate HC films. In this study, films were prepared by employing a static casting system via the breath figure technique. Polymers were dissolved in chloroform at a concentration of 5 mg mL<sup>-1</sup> and cast under a relative humidity of 70–90%. As expected, linear PMMA ( $M_w = 8.4$  kDa) and PS ( $M_w = 30$  kDa) have shown to be incapable of forming HC patterned films (**Figs 1a** and **2a**). In addition, no porous structure was observed from the film formed from **FP** alone under various humidities (**Fig. 1b**). This could be possibly due to the high fluorine content and the low glass transition temperature of **FP**. As observed in our recent study,<sup>[43]</sup> high fluorination ( $F > 50$  mol-%) led to less regular HC structures. The investigation of HC formation from PMMA and PS in the presence of **FP** as additive was then performed. **FP** was dissolved in chloroform at 5 mg mL<sup>-1</sup> and then added to PMMA solution at varying ratios. The resulting solutions were subsequently cast onto a planar surface under breath figure conditions, forming films which were analyzed by scanning electron microscopy (SEM) (**Fig. 1**).

Addition of 1 wt-% of **FP** to PMMA resulted in the formation of highly ordered HC films (**Fig. 1c**). The 2D fast Fourier transform (FFT) image (**Fig. 1c** inset) showed a uniform pattern consistent with a regular hexagonal arrangement, validating the formation of a HC pattern with a very narrow pore size distribution (**Fig. 1g**). This is considerably different from the results when PMMA was used solely (**Fig. 1a**). With increased levels of **FP** (5 and 10 wt-% i.e. **B1<sub>5</sub>** and **B1<sub>10</sub>**, respectively), as shown in **Fig. 1d, e**, highly ordered HC structures were formed, and their 2D FFT images display clear hexagonal arrangements. However, a further increase in **FP** content (15 wt-%, **B1<sub>15</sub>**) led to

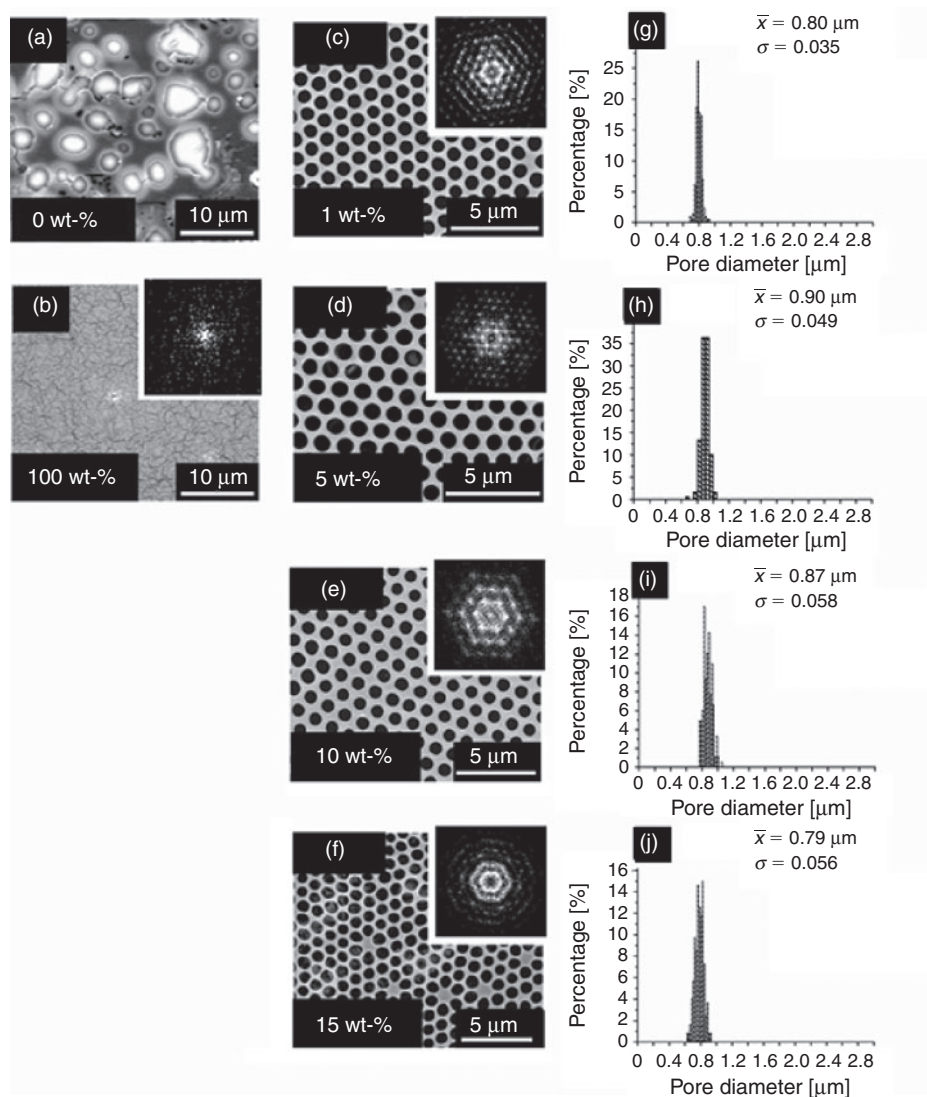


**Fig. 1.** SEM images of the breath figure films formed from (a) PMMA only, (b) FP only, and (c–f) mixtures of FP and PMMA at 1, 5, 10, and 15 wt-% FP (**B1**<sub>1</sub>, **B1**<sub>5</sub>, **B1**<sub>10</sub>, and **B1**<sub>15</sub>) and (g–j) their corresponding pore size distributions. The insets in (b–f) show the 2D FFT results. The mean ( $\bar{x}$ ) values and corresponding standard deviation ( $\sigma$ ) values are also presented.

a less regular HC pattern with the appearance of several defects (Fig. 1f). PMMA in the presence of 1 wt-% FP appeared to form the most regular HC film. The average pore size increased when the concentration of FP used increased from 1 to 5 wt-% and then decrease as the additive content increased. It is believed that at 1 wt-% FP, there is not enough hydrophobic polymer to stabilize the water droplet, and a faster precipitation rate occurs, leading to a smaller pore size. When the concentration was increased to 5 wt-%, the amount of FP was sufficient to stabilize the water droplets, thus a larger pore size was observed. However, with increasing amounts of FP, and hence higher contents of incorporated fluorine, the hydrophobicity of the polymer solution increased, leading to a faster solidification rate and hence a gradual reduction in pore size. These results are consistent with previously reported observations for fluorinated star polymers.<sup>[43]</sup>

The versatility of FP was further explored by adding it to PS at two different weight fractions: 1 wt-% (**B2**<sub>1</sub>) and 5 wt-% (**B2**<sub>5</sub>). The SEM images of the resultant PS-based porous structures are shown in Fig. 2.

Compared with the film formed from PS alone (Fig. 2a), sample **B2**<sub>1</sub> featured improved pore regularity with smaller pore sizes (Fig. 2c, e). A highly ordered HC patterned film was achieved from PS mixed with 5 wt-% additive (**B2**<sub>5</sub>) (Fig. 2d, f), where the 2D FFT image indicated the formation of a highly regular porous structure.

Such a significant improvement in forming HC films makes us question why linear polymers, which would normally not generate HC patterns, are able to form regular patterns in the presence of 1 wt-% FP only for PMMA (Fig. 1c) and 5 wt-% FP only for PS (Fig. 2d).

We subsequently conducted various analyses to investigate the physical property changes in the samples prepared with and without additive FP.

#### Physical Properties of PMMA and PMMA with Additive (**B1**<sub>1</sub>)

In order to ascertain the reasons for fluorinated additive (**B1**<sub>1</sub>) having such a significant effect on the HC formation, the physical properties of glass transition temperature ( $T_g$ ),

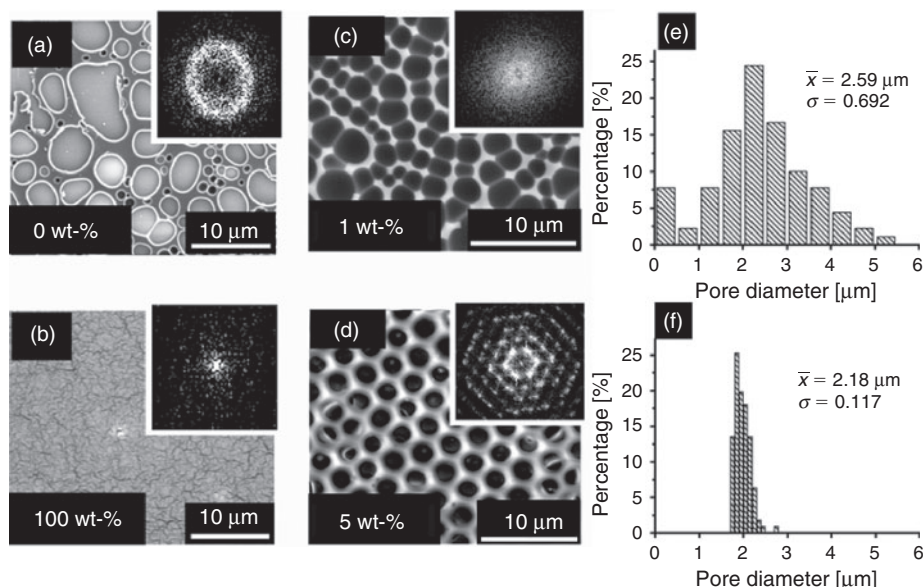


**Fig. 2.** SEM images of the breath figure films formed from (a) PS only, (b) FP only, and mixtures of FP and PS at (c) 1 wt-% FP (**B2<sub>1</sub>**) and (d) 5 wt-% FP (**B2<sub>5</sub>**). The insets in (a–d) show the 2D FFT results. Pore size distribution profiles of (e) **B2<sub>1</sub>** and (f) **B2<sub>5</sub>**.

Young's modulus ( $E$ ), interfacial tension of the oil–water interface ( $\gamma_{OW}$ ), polymer viscosity, and solidification rate were determined for the samples prepared without and with additive (**B1<sub>1</sub>**).

#### Polymer Glass Transition Temperature ( $T_g$ ) and Young's Modulus ( $E$ )

As shown in our previous studies, the glass transition temperature ( $T_g$ ) and Young's modulus ( $E$ ) were found to change with an increase in fluorine content of a polymer.<sup>[43,44]</sup> Compared with the parameters of the sample prepared from PMMA alone, both  $T_g$  (Table 1, Fig. S1, available online in the Supplementary Material) and  $E$  were lower for the sample prepared in the presence of 1 wt-% of FP (**B1<sub>1</sub>**) (Table 1). Our recent work showed that with smaller  $E$  values below 5.07 GPa, the cracking behaviour of HC films on non-planar surfaces could be improved.<sup>[44]</sup> Similarly, polymer sample **B1<sub>1</sub>** had a measured  $E$  of 4.76 (Fig. S2), and when it was cast onto a non-planar surface (regular transmission electron microscopy (TEM) grid), a perfect non-cracking HC film was formed. This result further validates our previous observations.

#### Interfacial Tension between Water and Polymer Solution

The interfacial tension ( $\gamma_{OW}$ ) of the polymer solutions was measured at the interface between water and polymer solution using the pendant drop technique.<sup>[45]</sup> The  $\gamma_{OW}$  values of the four polymer solutions containing 0, 1, 10, and 20 wt-% FP relative to PMMA dissolved in  $\text{CHCl}_3$  were measured. Measurements for each solution were conducted at varying concentrations by slowly injecting the polymer solution into the water phase, forming a stable pendant droplet (Fig. 3a). Images for each sample were captured (1 picture per second) and analyzed by Attension Theta (V 4.1.0), and the results are shown in Fig. 3.

The  $\gamma_{OW}$  of the polymer solutions decreased with increasing polymer solution concentrations; however, it was higher than that of pure chloroform. In addition,  $\gamma_{OW}$  increased with the increasing fluorine content. Hence, **B1<sub>20</sub>** (PMMA + 20 wt-% FP)

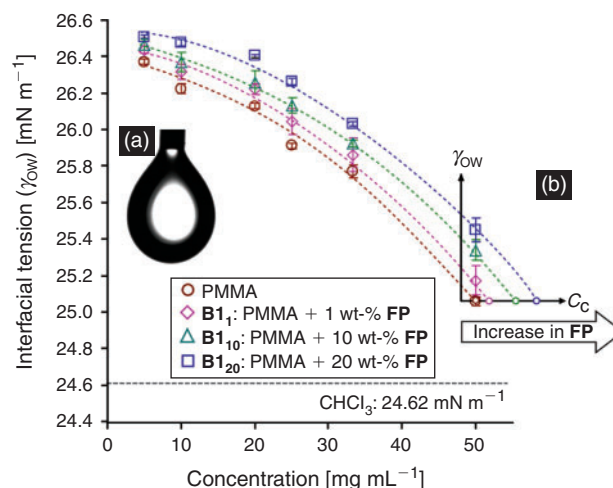


**Fig. 3.** Interfacial tension ( $\gamma_{OW}$ ) at the interface of polymer solution and water using the pendant drop technique (inset a). Critical coalescence concentration ( $C_C$ ) of the polymer samples at the same minimum  $\gamma_{OW}$  (inset b).

has the highest  $\gamma_{OW}$  among all four polymer solutions. It was noted that at a lower concentration the change in  $\gamma_{OW}$  was smaller. At a higher concentration, the change in  $\gamma_{OW}$  became larger. This trend indicates that with increasing polymer concentrations, there is a more significant difference in the interfacial tension between pure PMMA and FP added to PMMA. During HC formation, the polymer concentration increases as the solvent evaporates and a solid film is formed at the solution–water interface, which inhibits the coalescence process between droplets.<sup>[46]</sup> There is a relationship between the interfacial tension of the water droplets and the polymer solution concentration (Fig. 3). It is observed from this experiment that when FP is added to PMMA, the same interfacial tension is obtained at a higher polymer solution concentration (Fig. 3b).

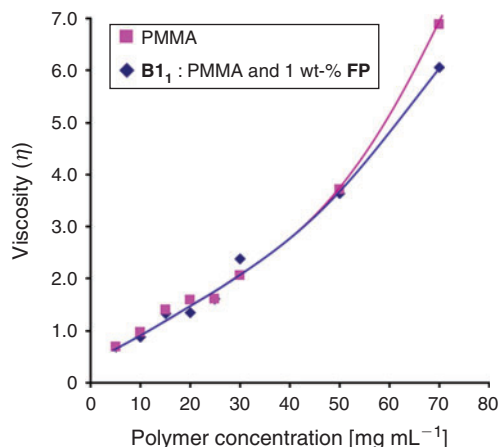


**Fig. 4.** Viscosity of the polymer solution versus polymer concentration: PMMA and polymer sample **B1<sub>1</sub>**.

#### Polymer Solution Viscosity Change

The viscosities of PMMA and PMMA mixed with 1 wt-% **FP** additive (**B1<sub>1</sub>**) were measured in toluene at varying concentrations using a Brookfield Rheometer. Toluene was chosen as the solvent for the viscosity measurements due to its lower volatility than chloroform and because HC films prepared from either solvent have similar characteristics. PMMA viscosity was initially measured by dissolving PMMA in toluene at a concentration of 70 mg mL<sup>-1</sup>, followed by successive dilution to different concentrations. As shown in Fig. 4, an increase in viscosity was observed as the concentration of PMMA both with and without 1 wt-% **FP** increased.

No significant difference was observed for the two samples at low polymer concentrations (<50 mg mL<sup>-1</sup>). However, at 70 mg mL<sup>-1</sup>, a clear difference in viscosity between PMMA and **B1<sub>1</sub>** became apparent (Fig. 4), with the sample **B1<sub>1</sub>** exhibiting a lower viscosity than PMMA alone. As the polymer concentration is expected to increase further during the breath figure process until solidification of the polymer occurs, the viscosity difference is expected to become more significant. This observation is in agreement with earlier results, which showed a decrease in  $E$  of the sample **B1<sub>1</sub>** when compared with that displayed by PMMA. This observation is well known in the plastics industry—small amount of additives (plasticisers) can be used to substantially change the flexibility of a polymer film such as the addition of polyvinyl chloride in plastic bag applications.<sup>[47]</sup>

In the case of HC formation when 1 wt% of **FP** is added to PMMA, there is a decrease in viscosity, which in turn leads to a quicker rearrangement of the water droplets into an ordered array, thereby facilitating HC film formation.

#### Polymer Solidification Rate

As a polymer solidification rate is related to its solubility, the solubilities of PMMA and **B1<sub>1</sub>** were determined by titration of a non-solvent into a polymer solution. A stock solution of PMMA in toluene (5 mg mL<sup>-1</sup>) was prepared, which is the same concentration as that of the casting solution. The solubility measurements were performed at room temperature (~25°C) by measuring light transmission through solutions using UV-visible spectroscopy, while a non-solvent (methanol) was titrated into the polymer solution until a cloudy point was observed. The resultant transmission (% $T$ ) is shown as a

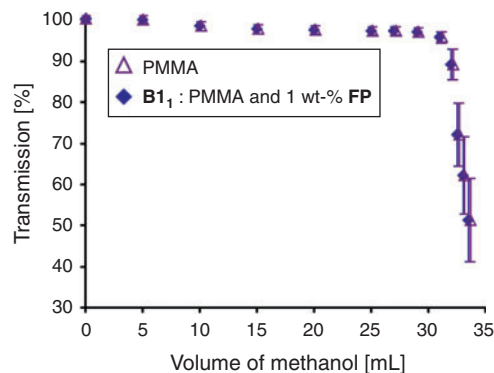


**Fig. 5.** Transmission of polymer solutions of PMMA and **B1<sub>1</sub>** measured by UV-visible spectroscopy ( $\lambda = 633$  nm).

function of methanol volume; a sudden drop in transmission was observed, indicating the solidification point (Fig. 5). It should be noted that the temperature during the UV-visible analysis remained constant, whereas during the Breath Figure process, the temperature significantly changes. Nevertheless, low levels of additive **FP** do not seem to have a significant impact on the polymer solidification behaviour.

#### Hypothesis on Influencing Factors Controlling HC Formation via Breath Figure Technique

The additive effect observed in this study raises important fundamental questions. With the addition of 1 wt-% **FP**, what properties of the polymer solution have been changed to facilitate the formation of HC films? How did these changes in the polymer properties make HC formation possible?

The mechanism of the breath figure process is not as simple as the approach to generate such interesting materials. Several detailed theories have been developed to explain the dynamic processes involved including diffused based models,<sup>[48]</sup> evaporation-induced convective assembly,<sup>[49,50]</sup> and Bénard–Marangoni convections.<sup>[51–53]</sup> The breath figure process is a complicated and dynamic process, which occurs as water vapour condenses to form water droplets within a polymer solution. It is known from previous studies that with the rapid evaporation of the volatile solvent, several parameters that affect coalescence change: (1) the viscosity of the casting solution increases dramatically, due to fast solvent evaporation; (2) the interfacial tension at the water–polymer interface decreases with increasing polymer concentrations;<sup>[53,54]</sup> (3) polymer solidification occurs, resulting in a polymer interfacial layer, which stabilizes the water and polymer phases, and thus retards water droplet coalescence;<sup>[53,54]</sup> and lastly (4) the magnitude of the capillary forces ( $F_T$ ) changes, thus influencing the self-assembly of water droplets.<sup>[55]</sup> In this study, a hypothesis is proposed based on a combination of these observed physical properties, which might be used to predict the formation of hexagonal patterned films from a new material. It was noted that there are two very important stages for water droplet formation during the breath figure process i.e. condensation and self-assembly.<sup>[53]</sup> During the condensation stage, the interfacial tension ( $\gamma_{OW}$ ) at the polymer solution and water interface is known to be a key factor for successful HC film formation.<sup>[34,54,56–60]</sup> During the self-assembly process, water droplets grow as a function of time, and the growth rate decreases with time due to increased viscosity and a decrease in temperature resulting from the rapid evaporation of solvent.<sup>[61]</sup> In other words, a higher polymer concentration leads

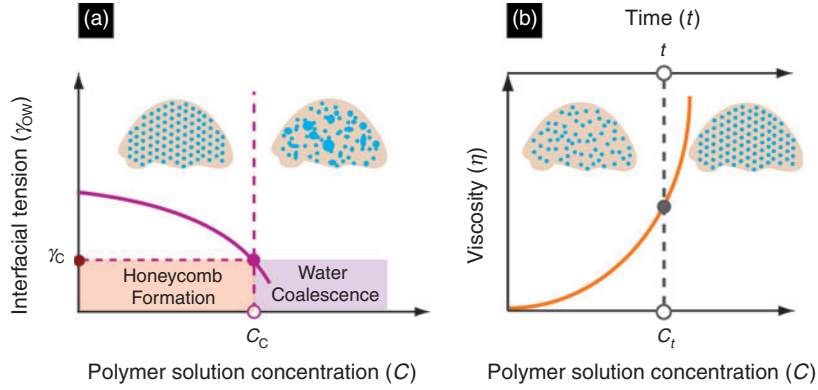


**Fig. 6.** (a) Influence of the interfacial tension ( $\gamma_{ow}$ ) and polymer concentration ( $C$ ) on water coalescence, where  $\gamma_c$  is the critical interfacial tension for water coalescence to occur and  $C_c$  is the critical coalescence concentration. (b) Influence of the polymer solution viscosity ( $\eta$ ) on water droplets arrangement as a function of time ( $t$ ) and polymer concentration ( $C$ ), where  $C_t$  is the critical self-assembly concentration for water droplet self-assembly.

to a slower water droplet growth rate. Moreover,  $\gamma_{ow}$  decreases with increasing polymer concentrations, thereby accelerating the rate of water droplet coalescence.<sup>[54]</sup> As a result of this phenomenon, the decrease in  $\gamma_{ow}$  eventually reaches a critical value ( $\gamma_c$ ), where the corresponding concentration is defined as the critical coalescence concentration ( $C_c$ ), beyond which point water coalescence occurs (Fig. 6a). When the interfacial tension approaches  $\gamma_c$ , water droplets become more unstable and coalescence can be triggered by external disturbances such as thermal shock, vibration, and dust.<sup>[62]</sup>

To avoid water droplet coalescence and thus form a HC film, it is desirable to have a high  $\gamma_{ow}$  and therefore a high  $C_c$ . Therefore, to prevent water droplet coalescence, the polymer concentration needs to be below  $C_c$  (Fig. 6a).

Parameter  $C_s$  is defined as the critical solidification concentration at which point polymer solidification occurs and water self-assembly ceases. If  $C_s$  occurs after  $C_c$  ( $C_c < C_s$ ), coalescence of the water droplets occurs (Fig. 7c). For regular ordered HC film formation,  $C_s$  needs to be below  $C_c$  to enable the droplets to be fixed before coalescence occurs (Fig. 7b).

On the other hand, with an increase in polymer concentration, the viscosity of the solution increases and the ability for water droplets to self-assemble decreases (Fig. 6b). In order to form a perfect HC pattern, water droplets need sufficient time to assemble into a hexagonally packed array. During the breath figure process, as solvent evaporation occurs, the polymer concentration ( $C$ ) increases and capillary forces ( $F_T$ ) are induced along with a rapid increase in the polymer solution viscosity ( $\eta$ ).  $F_T$  will decrease as the rate of solvent evaporation decreases as the temperature gradient decreases with time.<sup>[55]</sup> Here, time,  $t$ , is defined as the minimum time required for  $F_T$  to self-assemble water droplets into regular honeycomb patterns at a concentration defined as  $C_t$  (Fig. 6b). If  $C_s$  occurs before  $C_t$  (and even  $C_t$  occurs before  $C_c$ ), insufficient time for self-assembly leads to the water droplets structure being fixed in irregular patterns (Fig. 7a).

To prevent water droplet coalescence, the critical solidification concentration needs to occur before the critical coalescence concentration ( $C_s < C_c$ ). In addition, there needs to be sufficient time for the self-assembly of the water droplets into regular HC patterns with  $C_t$  occurring before  $C_s$  ( $C_t < C_s$ ). When considering all three parameters together, perfect HC film formation requires the following relationship:  $C_t < C_s < C_c$  (Fig. 7b). When  $C_s$

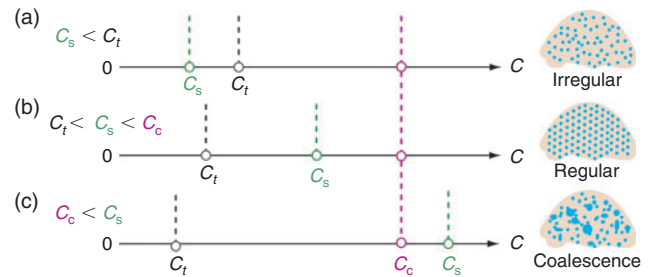


**Fig. 7.** Influence of critical polymer concentrations,  $C_s$ ,  $C_t$ , and  $C_c$ , on water droplet arrangement as a function of polymer concentration ( $C$ ): (a)  $C_s < C_t$ ; (b)  $C_t < C_s < C_c$ ; and (c)  $C_c < C_s$ .  $C_t$  is the critical self-assembly concentration for water droplet self-assembly;  $C_c$  is the theoretical critical coalescence concentration at which water coalescence occurs; and  $C_s$  is the critical solidification concentration at which the polymer solidifies.

occurs after  $C_c$  regardless where  $C_t$  is, water droplet coalescence will occur (Fig. 7c).

### Three-Parameter Hypothesis Applied to PMMA and B1

According to the proposed hypothesis, the most likely reason why linear PMMA itself does not form a HC structure is  $C_{s-PMMA} > C_{c-PMMA}$ . This means that water droplet coalescence at  $C_{c-PMMA}$  occurred before solidification at  $C_{s-PMMA}$ , resulting in a film with a chaotic porous structure (Fig. 8a). With the addition of FP additive to PMMA (Fig. 8b), the new solution has a lower viscosity at high polymer concentration (as observed in Fig. 4), which in turn reduces the expected time for rearrangement of the water droplets and hence  $C_t$ . The polymer sample B1 may have a similar solidification rate ( $C_{s-B1}$ ) to PMMA ( $C_{s-PMMA}$ ), as no difference in solidification measurement was observed. Yet, the interfacial tension of the sample was found to be higher than that displayed by PMMA (Fig. 3), resulting in  $C_{c-B1}$  being higher than  $C_{c-PMMA}$  and more importantly higher than  $C_{s-B1}$  (Fig. 8b), resulting in the solidification of the polymer before coalescence and thus the formation of a HC patterned film (Fig. 8b). When 5, 10, or 15 wt-% additive was added (Fig. 8c–e), the increasing amount of FP in the polymer sample enhances the interfacial tension, leading to  $C_c$  occurring at a progressively higher polymer concentration (Fig. 8c–e). Meanwhile, the increasing fluorine content in the polymer samples may also lead

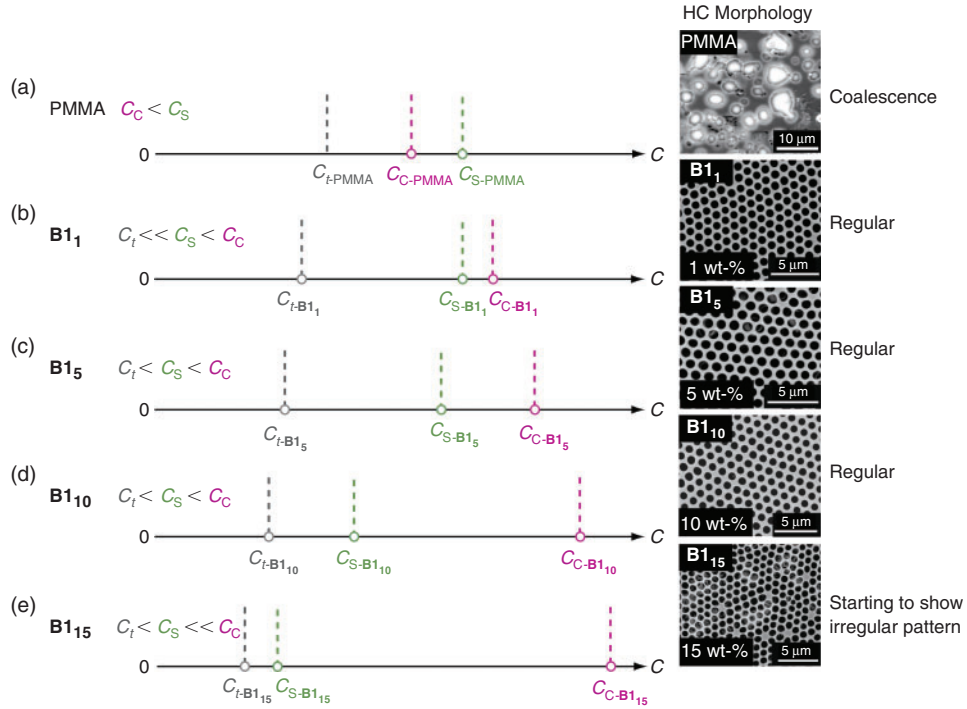


**Fig. 8.** Breath figure process based on the proposed mechanism and corresponding SEM images of (a) PMMA, (b) **B1**<sub>1</sub>, (c) **B1**<sub>5</sub>, (d) **B1**<sub>10</sub>, and (e) **B1**<sub>15</sub>. The critical coalescence concentrations for PMMA and the polymer samples are referred as  $C_{C-PMMA}$ , and  $C_{C-B1_1}$ ,  $C_{C-B1_5}$ ,  $C_{C-B1_{10}}$ , and  $C_{C-B1_{15}}$ , respectively; the critical solidification concentrations for PMMA and the polymer samples are referred as  $C_{S-PMMA}$ , and  $C_{S-B1_1}$ ,  $C_{S-B1_5}$ ,  $C_{S-B1_{10}}$ , and  $C_{S-B1_{15}}$ , respectively; and the critical self-assembly concentrations for PMMA and the polymer samples are referred as  $C_{I-PMMA}$ , and  $C_{I-B1_1}$ ,  $C_{I-B1_5}$ ,  $C_{I-B1_{10}}$ , and  $C_{I-B1_{15}}$ , respectively.

to a faster solidification rate due to its increased hydrophobicity. Therefore, their  $C_S$  may approach  $C_t$ , yet still remaining within the optimal range for forming regular HC structures (Fig. 8c, d). As the fluorine content in the mixture continues to increase,  $C_S$  decreases further and approaches  $C_t$ . This results in a porous pattern not fully stabilized before solidification and thus may contain some defects such as those seen for **B1**<sub>15</sub> (Fig. 8e).

In summary, the addition of 1–5 wt-% of FP additive resulted in an increased  $\gamma_{OW}$ , hence an increased  $C_C$ , no significant change or reduction in  $C_S$ , and a possible reduction in  $C_t$  to make  $C_S$  fall before  $C_C$  and after  $C_t$ . We believe that this dynamic process causes the three parameters of  $C_t$ ,  $C_C$ , and  $C_S$  to occur at different stages and hence gives different morphology outcomes. These parameters are dictated by the combination of precursors, for example, with or without additives. A combination of these changes are the likely mechanisms to effectively enable ordered HC film formation.

#### HC Film Formation from Linear PMMA and PS with Varying Molecular Weights

Regular HC film formation from linear PMMA and PS was reported to have molecular weight effects.<sup>[28,29]</sup> The critical molecular weight ( $M_w$ ) for linear PMMA and PS to form HC structures was reported as 102.6 kDa and 223.2 kDa, respectively. Interestingly, it was also reported that for linear PS, the maximum  $M_w$  for HC film formation is around 2000 kDa.<sup>[29]</sup> However, the reason behind this was never discussed. In general, the  $M_w$  of a linear polymer is related to its intrinsic viscosity ( $[\eta]$ ) by the Mark–Houwink–Sakurada equation.<sup>[63]</sup>

$$[\eta] = KM_w^a \quad (1)$$

where the constants  $K$  and  $a$  are dependent on the polymer, solvent, and temperature. Moreover, for a homogeneous linear polymer solution, the specific viscosity ( $\eta_{sp}$ ) is also related to  $[\eta]$ :<sup>[64]</sup>

$$\eta_{sp}(c) = [\eta]c + k_H([\eta]c)^2 + \dots \quad (2)$$

where  $c$  is the polymer concentration and  $k_H$  is the Huggins coefficient. Therefore, the viscosity of a polymer solution increases with the increasing intrinsic viscosity of a polymer. Research has shown that for linear PMMA and PS,<sup>[65,66]</sup> with a significant increase in  $M_w$ , the viscosity of PMMA and PS in solution increases dramatically.

With increased  $M_w$ , its influence on  $\gamma_{OW}$  is limited and  $C_C$  is not expected to change significantly. As the polymer solution becomes more viscous with increasing  $M_w$ , the time required for water droplets to self-assemble into regular arrangements increases (i.e. an increase in  $C_t$ ), whereas  $C_S$  will decrease dramatically. The three following scenarios then become apparent. At a high  $M_w$ , precipitation is fast as  $C_S$  is reduced dramatically below  $C_t$ , which in turn is increased due to an increase in viscosity, resulting in an irregular HC formation (Fig. 7a). At a medium  $M_w$ ,  $C_S$  is below  $C_C$  and above  $C_t$ , thus forming a regular HC structure (Fig. 7b). Whereas at a low  $M_w$ ,  $C_S$  is likely to be very high as the polymer does not readily precipitate.  $C_S$  is likely to be above  $C_C$ , causing water droplets to coalesce (Fig. 7c).

#### Conclusions

In this paper, we present the discovery of an additive (FP), which when added in small amounts was able to facilitate HC film formation of polymers otherwise unable to form regular HC

films by themselves. We examined the changes in the polymer solution viscosity ( $\eta$ ), polymer solidification rate, and interfacial tension ( $\gamma$ ) and determined that these were critical for HC film formation. We have proposed that these parameters relate directly to specific stages of the breath figure process, wherein the concentrations of the polymer solution are defined as  $C_b$ ,  $C_s$ , and  $C_c$ , respectively. Importantly, it was proposed that for successful HC formation  $C_i < C_s < C_c$  should apply. Although only qualitative measurements of these three parameters have been presented, they have been demonstrated to serve as a useful guide to designing future polymer systems for HC film formation. This theory has been used to explain why some materials and not others can form HC films. These findings are expected to significantly broaden the range of polymers that can successfully be used to form HC films.

## Experimental

### Materials

All materials were purchased from Sigma-Aldrich unless otherwise stated. 2-Bromoisobutryl bromide (98%), copper(I) bromide (CuBr) (98%), lithium bromide (LiBr) ( $\geq 99\%$ ), 1,6-hexanediol (99%),  $N,N,N',N'',N'''$ -pentamethyldiethylene-triamine (99%), sodium bicarbonate ( $\text{NaHCO}_3$ ), magnesium sulfate ( $\text{MgSO}_4$ ) (anhydrous,  $\geq 99.5\%$ ), hydrochloric acid (HCl) (ACS reagent, 37%), and tetrahydrofuran (THF) (anhydrous,  $\geq 99.9\%$ , inhibitor-free) were used without further purification. 2,2,3,3,3-Pentafluoropropyl acrylate (PFPA) ( $>97\%$ ) was purchased from Fluorochem and used as received. Activated neutral aluminium oxide ( $\text{Al}_2\text{O}_3$ ) was purchased from Merck. Triethylamine (TEA) (Chem-Supply, laboratory reagent (LR) grade) was distilled from  $\text{CaH}_2$  before use. Toluene (HPLC grade),  $N,N$ -dimethylformamide (DMF), dichloromethane ( $\text{CH}_2\text{Cl}_2$ ) (analytical reagent (AR) grade), chloroform ( $\text{CHCl}_3$ ) (AR grade), and methanol (MeOH; AR grade) were purchased from Chem-Supply and used as received. Deuterated chloroform ( $\text{CDCl}_3$ ) + 1% v/v tetramethylsilane (TMS) (D, 99.8%) was purchased from Cambridge Isotope Laboratories. Argon (UHP) was purchased from BOC, Australia. Carbon-coated copper TEM grids (300 mesh) were purchased from ProSciTech Pty Ltd.

### Methods

GPC was performed on a Shimadzu liquid chromatography system fitted with a Wyatt DAWN HELEOS LS detector ( $\lambda = 658$  nm), a Shimadzu RID-10 refractometer ( $\lambda = 633$  nm), and a Shimadzu SPD-20A UV-visible detector, using three identical Polymer Laboratories PLgel columns (5  $\mu\text{m}$ , MIXED-C) and DMF with 0.05 M LiBr (70°C; 1 mL  $\text{min}^{-1}$ ) as mobile phase. ASTRA software (Wyatt Technology Corp.) was used to process the data using either known differential index of refraction ( $dn/dc$ ) values or based upon 100% mass recovery of the polymer where the  $dn/dc$  value was unknown.  $^1\text{H}$  NMR spectroscopy analysis was performed on a Varian Unity Plus 400 MHz spectrometer. Deuterated chloroform ( $\text{CDCl}_3$ ) with 1% TMS (internal reference) was used as solvent. HC films were imaged by SEM using a FEI Quanta 200 ESEM FEG. Samples were pre-coated with gold using a Dynavac Mini sputter coater before imaging. Differential scanning calorimetry (DSC) was performed on a 2920 Modulated DSC (TA Instruments). TA Universal Analysis 2000 was used to process the data for determination of  $T_g$ . Each sample was heated and cooled twice at a heating rate of 10°C  $\text{min}^{-1}$  and the  $T_g$  values taken on

the second heating cycle. Atomic force microscopy (AFM) was performed on an Asylum Research MFP-3D AFM. Non-porous thin films were prepared by depositing 20  $\mu\text{L}$  of a polymer solution onto a clean microscope glass slide and allowing the solvent to evaporate at room temperature. The elastic modulus ( $E$ ) of these thin films was measured in force mode using pyramid-shaped silicon cantilevers (Model AC240Ts, 70 (50–90) kHz, 2 (0.5–4.4) N  $\text{m}^{-1}$ ; AC200Ts, 115 (75–175) kHz, 9.7 (4.0–22.3) N  $\text{m}^{-1}$ ; AC160Ts, 300 (200–400) kHz, 42 (12–103) N  $\text{m}^{-1}$ ; Asylum Research). The Hertzian contact mechanics model<sup>[67–69]</sup> was applied on approach curves to obtain  $E$ . Image-Pro® software was employed to analyze the SEM images of the HC films. Interfacial tension measurements were performed on a KSV Instrument CAM 200, and results were analyzed by Attension Theta (V 4.1.0). Polymer solution viscosities were measured on a Brookfield DV-III ULTRA programmable rheometer at various shear rates ranging from 0.17 to 2.00  $\text{s}^{-1}$ . Measurements were recorded for each concentration once shear thinning had occurred, and the recorded viscosity (cP) (Fig. 4) was independent of the shear rate. Polymer solidification rates were measured on a Varian CARY 50 Bio-UV-visible spectrophotometer.

### Synthesis of Di-Functional Initiator 1

A solution of 1,6-hexanediol (2.00 g, 16.9 mmol) and TEA (5.90 mL, 42.3 mmol) in anhydrous THF (16 mL) was cooled to 0°C in an ice-bath under argon and treated dropwise with 2-bromoisobutryl bromide (5.02 g, 40.6 mmol) over 15 min whilst maintaining the temperature below 0°C, followed by stirring for another 30 min. The reaction mixture was allowed to warm to room temperature and stirred for 4 h. The organic solution was washed with 2 M HCl (40 mL), 2 M  $\text{NaHCO}_3$  (2  $\times$  30 mL), and water (30 mL), dried ( $\text{MgSO}_4$ ), filtered, and concentrated under vacuum (20 mbar, 50°C). The residue was passed through basic alumina to afford a viscous yellow oil (5.60 g, 80%).  $\delta_{\text{H}}$  ( $\text{CDCl}_3$ , 400 MHz) 1.41 (q,  $J$  3.6,  $\text{CH}_2$ ), 1.68 (q,  $J$  6.5,  $\text{CH}_2$ ), 1.90 (s,  $\text{CH}_3$ ), 4.15 (t,  $J$  6.5,  $\text{CH}_2\text{O}$ ).  $\delta_{\text{C}}$  ( $\text{CDCl}_3$ , 50 MHz) 171.6 (C=O), 65.8 ( $\text{CH}_2\text{O}$ ), 55.9 (C–Br), 30.7 ( $\text{CH}_3$ ), 28.2 ( $\text{CH}_2$ ), 25.4 ( $\text{CH}_2$ ).

### Conventional Polymerization of Methyl Methacrylate

A 50-mL Schlenk tube (oven-dried at 110°C for 48 h) was fitted with a stirrer bar and a solution of MMA (6.1 g, 60.9 mmol), and 2,2'-azobis(2-methylpropionitrile) (0.1 g, 0.61 mmol) in toluene (13.8 mL) was added. The reaction mixture was purged with nitrogen, then heated at 60°C in an oil bath for 4 h. The solution mixture was precipitated into methanol, collected, and dried under vacuum (50°C) to afford linear PMMA as a white solid (4.96 g, 80%).  $\delta_{\text{H}}$  ( $\text{CDCl}_3$ , 400 MHz) 0.81–0.94 (m,  $\text{CH}_3$ ), 1.50–2.60 (m, CH &  $\text{CH}_2$ ), 3.30–3.96 (m,  $\text{OCH}_3$ ).

### Synthesis of Fluorinated Linear Gradient Polymer (FP)

A 50-mL Schlenk tube (oven-dried at 110°C for 48 h) was fitted with a stirrer bar and initiator 1 (0.05 g, 0.12 mmol, 1 equiv.), and PMDTA (0.025 mL, 0.12 mmol, 1 equiv.), PFPA (0.186 mL, 1.20 mmol, 10 equiv.), MMA (0.821 mL, 10.80 mmol, 90 equiv.), and toluene (1.80 mL) were added. The mixture was subjected to three freeze–pump–thaw cycles, then back-filled with argon. The Schlenk tube was then immersed again in liquid  $\text{N}_2$ , and once the solution had frozen, CuBr (0.017 g, 0.12 mmol) was added. Another three freeze–pump–thaw cycles were performed, and then the Schlenk tube was

back-filled with argon and left at room temperature with stirring for 10 min to ensure homogeneity. The reaction mixture was then heated at 65°C in an oil bath for 6 h under an atmosphere of argon. An aliquot (0.2 mL) was taken via a gas-tight syringe at  $t_0$  and after 6 h to determine monomer conversion. The reaction mixture was diluted with  $\text{CHCl}_3$  (3 mL) and passed through a plug of basic  $\text{Al}_2\text{O}_3$  to remove the copper catalyst. The filtrate was precipitated into methanol, collected, and dried under vacuum (0.1 mbar, 50°C) to afford linear gradient fluorinated polymer **FP** as a white solid (1.89 g, 63.0%).  $\delta_{\text{H}}$  ( $\text{CDCl}_3$ , 400 MHz) 0.81–0.94 (m,  $\text{CH}_3$ ), 1.50–2.60 (m, CH &  $\text{CH}_2$ ), 3.30–3.96 (m,  $\text{OCH}_3$ ), 4.30–4.70 (m,  $\text{OCH}_2$ ).

#### Flat Surface Casting

HC films were prepared using the static casting method. The casting environment was first stabilized at  $\sim 30^\circ\text{C}$ , with varying relative humidities from  $(70 \pm 5)\%$  up to  $(90 \pm 5)\%$ . Polymer solutions with a concentration of  $5 \text{ mg mL}^{-1}$  (20  $\mu\text{L}$ ) in  $\text{CHCl}_3$  were then injected onto circular glass coverslips, and the solvent and water were left to evaporate.

#### Non-Planar Surface Casting

A TEM grid was placed on a glass coverslip. Then, a drop (20  $\mu\text{L}$ ) of polymer solution ( $5 \text{ mg mL}^{-1}$  in  $\text{CHCl}_3$ ) was cast onto this grid under the same casting conditions used as above and left to dry. Analysis was performed using SEM imaging as described above.

#### Supplementary Material

The DSC trace and SEM images of honeycomb films from both PMMA and the PMMA blended with 1 wt-% **FP** (**B1**) are available from the Journal's website.

#### Acknowledgements

The authors wish to acknowledge CSIRO and The University of Melbourne for providing scholarships to Mr. Z. Zhang. The authors also wish to thank the Electron Microscopy Unit at the Bio21 Institute (The University of Melbourne) for assistance with SEM analysis and Dr A. Blencowe (The University of Melbourne) for the supply and analysis of the ATRP initiator **I**.

#### References

- [1] C. Cheng, Y. Tian, Y. Shi, R. Tang, F. Xi, *Macromol. Rapid Commun.* **2005**, *26*, 1266. doi:10.1002/MARC.200500268
- [2] T. Hayakawa, S. Horiuchi, *Angew. Chem., Int. Ed.* **2003**, *42*, 2285. doi:10.1002/ANIE.200219877
- [3] B. de Boer, U. Stalmach, H. Nijland, G. Hadziioannou, *Adv. Mater.* **2000**, *12*, 1581. doi:10.1002/1521-4095(200011)12:21<1581::AID-ADMA1581>3.3.CO;2-I
- [4] W. Wang, C. Du, X. Wang, X. He, J. Lin, L. Li, S. Lin, *Angew. Chem., Int. Ed.* **2014**, *53*, 12116. doi:10.1002/ANIE.201407230
- [5] L. Song, R. K. Bly, J. N. Wilson, S. Bakbak, J. O. Park, M. Srinivasarao, U. H. Bunz, *Adv. Mater.* **2004**, *16*, 115. doi:10.1002/ADMA.200306031
- [6] T. Nishikawa, J. Nishida, R. Ookura, S.-I. Nishimura, S. Wada, T. Karino, M. Shimomura, *Mater. Sci. Eng., C* **1999**, *8–9*, 495. doi:10.1016/S0928-4931(99)00075-2
- [7] L.-W. Zhu, Y. Ou, L. S. Wan, Z. K. Xu, *J. Phys. Chem. B* **2014**, *118*, 845. doi:10.1021/JP4114392
- [8] A. E. Saunders, J. L. Dickson, P. S. Shah, M. Y. Lee, K. T. Lim, K. P. Johnston, B. A. Korgel, *Phys. Rev. E: Stat., Nonlinear, Soft Matter Phys.* **2006**, *73*, 031608. doi:10.1103/PHYSREVE.73.031608
- [9] C. X. Cheng, Y. Tian, Y. Q. Shi, R. P. Tang, F. Xi, *Langmuir* **2005**, *21*, 6576. doi:10.1021/LA050187D
- [10] J. Chen, X. Yan, Q. Zhao, L. Li, F. Huang, *Polym. Chem.* **2012**, *3*, 458. doi:10.1039/C1PY00438G
- [11] G. Widawski, M. Rawiso, B. Francois, *Nature* **1994**, *369*, 387. doi:10.1038/369387A0
- [12] H. Sun, H. Li, W. Bu, M. Xu, L. Wu, *J. Phys. Chem. B* **2006**, *110*, 24847. doi:10.1021/JP064535B
- [13] M. H. Stenzel, T. P. Davis, A. G. Fane, *J. Mater. Chem.* **2003**, *13*, 2090. doi:10.1039/B304204A
- [14] L. A. Connal, R. Vestberg, P. A. Gurr, C. J. Hawker, G. G. Qiao, *Langmuir* **2008**, *24*, 556. doi:10.1021/LA702495P
- [15] L. A. Connal, R. Vestberg, C. J. Hawker, G. G. Qiao, *Adv. Funct. Mater.* **2008**, *18*, 3315. doi:10.1002/ADFM.200800333
- [16] L. A. Connal, R. Vestberg, C. J. Hawker, G. G. Qiao, *Adv. Funct. Mater.* **2008**, *18*, 3706. doi:10.1002/ADFM.200800568
- [17] L. A. Connal, *Aust. J. Chem.* **2007**, *60*, 794. doi:10.1071/CH07137
- [18] Z. Zhang, X. J. Hao, P. A. Gurr, A. Blencowe, T. C. Hughes, G. G. Qiao, *Aust. J. Chem.* **2012**, *65*, 1186. doi:10.1071/CH12252
- [19] P. Tang, J. Hao, *J. Colloid Interface Sci.* **2009**, *333*, 1. doi:10.1016/J.JCIS.2008.12.036
- [20] Y. Yu, Y. Ma, *Soft Matter* **2011**, *7*, 884. doi:10.1039/C0SM01346C
- [21] M. Lomoschitz, S. Edinger, G. Bauer, G. Friedbacher, U. Schubert, *J. Mater. Chem.* **2010**, *20*, 2075. doi:10.1039/B927433B
- [22] X. Jiang, T. Zhang, L. Xu, C. Wang, X. Zhou, N. Gu, *Langmuir* **2011**, *27*, 5410. doi:10.1021/LA200375T
- [23] L.-S. Wan, L.-W. Zhu, Y. Ou, Z.-K. Xu, *Chem. Commun.* **2014**, *50*, 4024. doi:10.1039/C3CC49826C
- [24] H. Bai, C. Du, A. Zhang, L. Li, *Angew. Chem., Int. Ed.* **2013**, *52*, 12240. doi:10.1002/ANIE.201303594
- [25] E. Ferrari, P. Fabbri, F. Pilati, *Langmuir* **2011**, *27*, 1874. doi:10.1021/LA104500J
- [26] L. A. Connal, P. A. Gurr, G. G. Qiao, D. H. Solomon, *J. Mater. Chem.* **2005**, *15*, 1286.
- [27] L.-W. Zhu, B.-H. Wu, L.-S. Wan, Z.-K. Xu, *Polym. Chem.* **2014**, *5*, 4311. doi:10.1039/C4PY00206G
- [28] J. Peng, Y. Han, J. Fu, Y. Yang, B. Li, *Macromol. Chem. Phys.* **2003**, *204*, 125. doi:10.1002/MACP.200290068
- [29] J. Peng, Y. Han, Y. Yang, B. Li, *Polymer* **2004**, *45*, 447. doi:10.1016/J.POLYMER.2003.11.019
- [30] L.-S. Wan, J.-W. Li, B.-B. Ke, Z.-K. Xu, *J. Am. Chem. Soc.* **2012**, *134*, 95. doi:10.1021/JA2092745
- [31] A. Muñoz-Bonilla, E. Ibarboure, V. Bordege, M. Fernández-García, J. Rodríguez-Hernández, *Langmuir* **2010**, *26*, 8552. doi:10.1021/LA904565D
- [32] A. Muñoz-Bonilla, E. Ibarboure, E. Papon, J. Rodriguez-Hernandez, *Langmuir* **2009**, *25*, 6493. doi:10.1021/LA9003214
- [33] A. S. de León, A. del Campo, M. Fernández-García, J. Rodríguez-Hernández, A. Muñoz-Bonilla, *Langmuir* **2014**, *30*, 6134. doi:10.1021/LA5011902
- [34] L.-S. Wan, B.-B. Ke, J. Zhang, Z.-K. Xu, *J. Phys. Chem. B* **2012**, *116*, 40. doi:10.1021/JP208115U
- [35] T. Ponnusamy, L. B. Lawson, L. C. Freytag, D. A. Blake, R. S. Ayyala, V. T. John, *Biomater* **2012**, *2*, 77. doi:10.4161/BIOM.20390
- [36] Y. Fukuhira, E. Kitazono, T. Hayashi, H. Kaneko, M. Tanaka, M. Shimomura, Y. Sumi, *Biomaterials* **2006**, *27*, 1797. doi:10.1016/J.BIOMATERIALS.2005.10.019
- [37] L. A. Connal, R. Vestberg, P. A. Gurr, C. J. Hawker, G. G. Qiao, *Langmuir* **2008**, *24*, 556. doi:10.1021/LA702495P
- [38] M. H. Stenzel-Rosenbaum, T. P. Davis, A. G. Fane, V. Chen, *Angew. Chem.* **2001**, *113*, 3536. doi:10.1002/1521-3757(200109)113:18<3536::AID-ANGE3536>3.0.CO;2-6
- [39] X. Zhang, J. Ren, H. Yang, Y. He, J. Tan, G. G. Qiao, *Soft Matter* **2012**, *8*, 4314. doi:10.1039/C2SM07267J
- [40] F. Pilati, M. Montecchi, P. Fabbri, A. Synytska, M. Messori, M. Toselli, K. Grundke, D. Pospiech, *J. Colloid Interface Sci.* **2007**, *315*, 210. doi:10.1016/J.JCIS.2007.06.046
- [41] A. S. de León, A. del Campo, M. Fernández-García, J. Rodríguez-Hernández, A. Muñoz-Bonilla, *Langmuir* **2012**, *28*, 9778. doi:10.1021/LA3013188

- [42] N. V. Tsarevsky, K. Matyjaszewski, *RSC Polym. Chem. Ser.* **2013**, *4*, 287. doi:10.1039/9781849737425-00287
- [43] Z. Zhang, T. C. Hughes, P. A. Gurr, A. Blencowe, H. Uddin, X. J. Hao, G. G. Qiao, *Polymer* **2013**, *54*, 4446. doi:10.1016/J.POLYMER.2013.06.033
- [44] Z. Zhang, T. C. Hughes, P. A. Gurr, A. Blencowe, X. J. Hao, G. G. Qiao, *Adv. Mater.* **2012**, *24*, 4327. doi:10.1002/ADMA.201200877
- [45] A. Adamson, *Physical Chemistry of Surfaces, 3rd Ed.* **1976** (Wiley: New York, NY).
- [46] O. Pitois, B. François, *Colloid Polym. Sci.* **1999**, *277*, 574. doi:10.1007/S003960050427
- [47] M. Rahman, C. S. Brazel, *Prog. Polym. Sci.* **2004**, *29*, 1223. doi:10.1016/J.PROGPOLYMSCI.2004.10.001
- [48] V. Sharma, L. Song, R. L. Jones, M. S. Barrow, P. R. Williams, M. Srinivasarao, *Europhys. Lett.* **2010**, *91*, 38001. doi:10.1209/0295-5075/91/38001
- [49] M. Shimomura, T. Sawadaishi, *Curr. Opin. Colloid Interface Sci.* **2001**, *6*, 11. doi:10.1016/S1359-0294(00)00081-9
- [50] N. Maruyama, T. Koito, J. Nishida, T. Sawadaishi, X. Cieren, K. Ijio, O. Karthaus, M. Shimomura, *Thin Solid Films* **1998**, *327–329*, 854. doi:10.1016/S0040-6090(98)00777-9
- [51] E. Ferrari, P. Fabbri, F. Pilati, *Langmuir* **2011**, *27*, 1874. doi:10.1021/LA104500J
- [52] L. Cui, Y. Han, *Langmuir* **2005**, *21*, 11085. doi:10.1021/LA0511135
- [53] O. Pitois, B. François, *Eur. Phys. J. B* **1999**, *8*, 225. doi:10.1007/S100510050685
- [54] Y. Fukuhira, H. Yabu, K. Ijio, M. Shimomura, *Soft Matter* **2009**, *5*, 2037. doi:10.1039/B821183C
- [55] N. Maruyama, O. Karthaus, K. Ijio, M. Shimomura, T. Koito, S. Nishimura, T. Sawadaishi, N. Nishi, S. Tokura, *Supramol. Sci.* **1998**, *5*, 331. doi:10.1016/S0968-5677(98)00027-3
- [56] A. Bolognesi, C. Mercogliano, S. Yunus, M. Civardi, D. Comoretto, A. Turturro, *Langmuir* **2005**, *21*, 3480. doi:10.1021/LA047427U
- [57] M. S. Park, W. Joo, J. K. Kim, *Langmuir* **2006**, *22*, 4594. doi:10.1021/LA053009T
- [58] X. Xiong, W. Zou, Z. Yu, J. Duan, X. Liu, S. Fan, H. Zhou, *Macromolecules* **2009**, *42*, 9351. doi:10.1021/MA9018119
- [59] M. Kojima, Y. Hirai, H. Yabu, M. Shimomura, *Polym. J.* **2009**, *41*, 667. doi:10.1295/POLYMJ.PJ2009027
- [60] A. Zhang, C. Du, H. Bai, Y. Wang, J. Wang, L. Li, *ACS Appl. Mater. Interfaces* **2014**, *6*, 8921. doi:10.1021/AM5016952
- [61] O. Pitois, B. François, *Colloid Polym. Sci.* **1999**, *277*, 574. doi:10.1007/S003960050427
- [62] A. Vrij, *Discuss. Faraday Soc.* **1966**, *42*, 23. doi:10.1039/DF9664200023
- [63] C. Tanford, *Physical Chemistry of Macromolecules* **1961** (Wiley: New York, NY).
- [64] H. Morawetz, *Macromolecules in Solution, 2nd Ed.* **1975** (Wiley, New York, NY).
- [65] P. Gupta, C. Elkins, T. E. Long, G. L. Wilkes, *Polymer* **2005**, *46*, 4799. doi:10.1016/J.POLYMER.2005.04.021
- [66] J. Jungnickel, F. Weiss, *J. Polym. Sci., Polym. Phys. Ed.* **1961**, *49*, 437.
- [67] H. Hertz, *J. Reine Angew. Math.* **1882**, *92*, 156.
- [68] A.-Y. Jee, M. Lee, *Polym. Test.* **2010**, *29*, 95. doi:10.1016/J.POLYMERTESTING.2009.09.009
- [69] M. J. Rosenbluth, W. A. Lam, D. A. Fletcher, *Biophys. J.* **2006**, *90*, 2994. doi:10.1529/BIOPHYSJ.105.067496